Composites Science Technology, vol 70, 2010, 193-199

The tensile fatigue behaviour of a silica nanoparticle-modified glass fibre reinforced epoxy composite

C.M. Manjunatha *, A.C. Taylor, A.J. Kinloch,

Department of Mechanical Engineering, Imperial College London, South Kensington Campus, London SW7 2AZ, U.K.

S. Sprenger

Nanoresins AG, Charlottenburger Strasse 9, 21502 Geesthacht, Germany

Abstract

An anhydride-cured thermosetting epoxy polymer was modified by incorporating 10 wt.% of well-dispersed 20 nm diameter silica nanoparticles. The stress-controlled tensile fatigue behaviour at a stress ratio of R = 0.1 was investigated for bulk specimens of the neat and the silica-modified epoxy. The addition of the silica nanoparticles increased the fatigue life by about three to four times. The neat and the nanoparticle-modified epoxy resins were used to fabricate glass fibre reinforced plastic (GFRP) composite laminates by resin infusion under flexible tooling (RIFT). Tensile fatigue tests were performed on these composites, during which the matrix cracking and stiffness degradation was monitored. The fatigue life of the GFRP composite was increased by about three to four times due to the silica nanoparticles. Suppressed matrix cracking and a reduced crack propagation rate in the nanoparticle-modified matrix were observed to contribute towards the enhanced fatigue life of the composite containing the silica nanoparticles.

Keywords:

A. Nano Composites; A. Polymer Matrix Composites (PMCs); B. Fatigue; B. Matrix Cracking;

* Corresponding author: Tel.: +44 20 7594 7090; Fax: +44 20 7594 7017

E-mail address: manjucm@nal.res.in (CM Manjunatha)

1. Introduction

Fibre reinforced plastic (FRP) composites are widely used in ship hull, airframe and wind turbine structural applications due to their high specific strength and stiffness. The components in such structures invariably experience various types of constant- and variable-amplitude fatigue loads in service. Safe operation of these structures for the designed lifetime requires that composite materials, in addition to their good static mechanical properties, need to have high fracture toughness and good fatigue-resistance.

The majority of engineering composite materials consist of a thermosetting epoxy matrix reinforced by continuous glass or carbon fibres. The epoxy, when polymerised, is an amorphous and highly cross-linked material. This cross-linked microstructure results in many useful properties such as a high modulus and failure strength, low creep etc.. However, it also leads to an undesirable property whereby the polymer is relatively brittle and has a poor resistance to crack initiation and growth. This will affect the overall fatigue and fracture performance of FRP composites with this matrix.

One of the ways to enhance the mechanical properties of FRPs is to improve the properties of the epoxy matrix by incorporating a second phase of particles into the resin. Polymeric nanocomposites, where at least one of the dimensions of the particulate material is less than 100 nm, have shown significant improvements in mechanical properties, e.g. [1,2]. Various types of particulate, fibrous and layered nanoparticles have been employed for both bulk polymers and fibre composites [3-13].

The beneficial effect of silica nanoparticles on the fracture toughness of epoxies and FRPs has been widely reported [3-10]. However, detailed studies on the fatigue behaviour of particle toughened nanocomposites are limited, e.g. [14]. Hence, the main aim of this investigation was to study the stress-controlled constant-amplitude tensile fatigue behaviour of a glass fibre reinforced plastic (GFRP) composite with a silica nanoparticle-modified epoxy matrix. Emphasis was placed on understanding the micro-mechanisms of the fatigue damage processes.

2. Experimental

2.1 Materials and processing

The materials were based upon a single-component hot-cured epoxy formulation. The epoxy resin was a standard diglycidyl ether of bisphenol A (DGEBA) with an epoxy equivalent weight (EEW) of 185 g/mol, 'LY556' supplied by Huntsman, Duxford, UK. The silica (SiO_2) nanoparticles were obtained as a colloidal silica sol with a concentration of 40 wt.% in DGEBA epoxy resin (EEW = 295 g/mol) as 'Nanopox F400' from Nanoresins, Geesthacht, Germany. The curing agent was an accelerated methylhexahydrophthalic acid anhydride, 'Albidur HE 600' (EEW = 170 g/mol) also from Nanoresins. The E-glass fibre cloth was a non-crimp-fabric with two layers of fibres arranged in a ±45° pattern with an areal weight of 450 g/m^2 from SP Systems, Newport, UK.

The DGEBA epoxy resin was weighed and degassed at 50 °C and -1 atm. The required quantity of silica nanoparticle-modified epoxy resin to give 10 wt.% of silica in the final formulation was also weighed and degassed. These were mixed together, a stoichiometric amount of curing agent was added, and the mixture was stirred and degassed. The resin mixture was then used to prepare both bulk epoxy sheets and GFRP composites. Typically, to prepare 500 ml (589 g) of 10 wt.% silica nanoparticle-modified resin, about 150 g of Nanopox, 184 g of LY556 and 255 g of HE600 was used.

To manufacture the bulk epoxy sheets, the resin mixture was poured into release-coated steel moulds. The filled moulds were placed in a circulating air oven. The temperature was ramped to 100 °C at 1 °C/min, and the epoxy was cured for 2 hours. The temperature was then ramped to 150 °C at 1 °C/min and the plate was post-cured for 10 hours. An atomic force microscope (AFM) image of the silica nanoparticle-modified epoxy polymer, obtained as described in [4], is shown in Fig. 1. This shows that the silica particles are about 20 nm in diameter and are evenly distributed in the epoxy.

The GFRP composite laminates were manufactured by resin infusion under flexible tooling (RIFT) [14]. E-glass fibre non-crimp fabric pieces, about 330 mm square, were cut and laid up in a quasi-isotropic sequence $[(+45/-45/90/0)_s]_2$ with a fluid distribution mesh. The resin mixture was infused

into the glass-cloth lay-up at 50 °C and -1 atm. Once the infusion was complete, the laminate was cured using the same cure cycle as the bulk plates, maintaining the vacuum throughout the curing process. The resulting GFRP composite laminates (neat and with silica nanoparticle-modified epoxy matrix) were about 2.5 - 2.7 mm thick, and had a fibre volume fraction of about 57%.

2.2 Tensile properties

The tensile properties of the bulk epoxies and GFRP composites were determined according to the ASTM D638 [16] and ASTM D3039 [17] test standard specifications respectively. Schematic drawings of the test specimens are shown in Fig. 2. The tensile tests were performed using a 100 kN computer-controlled screw-driven test machine with a constant crosshead speed of 1 mm/min. The average tensile properties, determined from five tests on each material, are shown in Table 1.

As observed in earlier investigations [4,5], the addition of silica nanoparticles increased the tensile strength and modulus of both the bulk epoxy and the GFRP composite. The ultimate tensile strength (UTS) increased by about 19% and 5%, whereas the modulus increased by about 17% and 7% in the bulk epoxy and GFRP composite respectively. Although the increases due to the addition of the nanoparticles are significant for the bulk epoxy, they are not significant for the GFRP as the composite properties are fibre-dominated.

2.3 Fatigue Testing

The fatigue test specimens, as shown in Fig. 2, were prepared from the bulk epoxy sheet and GFRP composite laminate. The sharp edges of the bulk epoxy test specimens were slightly rounded off with emery paper before testing, to avoid any stress concentration effect. The fatigue tests were performed as per the ASTM D3479M test standard [18], using a 25 kN computer-controlled servo-hydraulic test machine. The tests were conducted at a stress ratio (R) of σ_{min} / σ_{max} = 0.1 with a sinusoidal waveform at a frequency of ν = 1 to 3 Hz. The test frequency was kept below 3 Hz to prevent thermal effects which lead to reduced fatigue lives [19-21].

The load versus displacement data for one complete fatigue cycle was captured at regular intervals during the fatigue test, and the specimen stiffness was calculated [22]. About 50 pairs of load/displacement data in the central portion of the rising half of the fatigue cycle were used to perform the regression analysis. For the purpose of comparison, the normalised stiffness of the specimen was defined as the ratio of the initial stiffness (obtained in the first cycle) to the measured stiffness at any given fatigue cycle.

2.4 Measurement of crack density

Due to the translucent nature of the GFRP composite, the development of fatigue damage (matrix cracks and delaminations) was visible in the gauge section of the specimen using transmitted light during testing. Detailed investigation of matrix cracking was performed during one of the fatigue tests (at σ_{max} = 150 MPa) for both the neat and silica nanoparticle-modified GFRP composites.

An area at the centre of the gauge section of the test specimen, about 25 mm square, was marked. The specimen was mounted in the test machine and the cyclic loading was applied. After the application of a specified number of load cycles, the test was stopped, the specimen was dismounted and the matrix cracks in the marked area were photographed using transmitted light. The specimen was then re-mounted and the test restarted. This procedure was continued until the specimen failed.

A typical sequence of photographs obtained for the GFRP composite with the neat epoxy matrix is shown in Fig. 3. The virgin sample with no matrix cracks is on the far left. The polyester binding yarns in both 0° and ±45° directions can be readily seen as faint thick lines, but the E-glass fibres are not visible. With increasing number of cycles, cracks develop in the ±45° and 90° directions and become visible as dark lines. The higher the number of fatigue cycles, the greater the number of cracks that are formed. Similar observations of the matrix cracking sequence in a GFRP composite under fatigue has been reported previously [23].

Although cracks in the 90° ply were observed in some images, due to greater depth of this ply from the surface, they could not be consistently observed in all the photographs. Gagel et al [23]

observed that the stiffness of the composite in the first two stages of the fatigue life correlates strongly with the ±45° crack density and more weakly with the density of 90° cracks. Hence, only ±45° cracks were considered for the analysis in this investigation.

For the purpose of the analysis the crack density (CD), defined as the number of cracks per unit length, was determined by counting the visible cracks in the ±45° directions on an arbitrarily chosen line drawn on the images. Six such measurements were made on each of the photographs and the average CD was obtained. It may be noted that there is an uncertainty on the accuracy of such measurements as the depth of focus may influence the CD measurements via transmitted light photography. Hence, the CD measurements are used only for comparative statements.

3. Results and discussion

3.1 Fatigue behaviour of bulk epoxy

The constant-amplitude, tension-tension, cyclic-fatigue test results obtained for the neat and silica nanoparticle-modified bulk epoxy polymers are shown in Fig. 4. It may be clearly seen that, for a given maximum cyclic stress, the fatigue life of the nanoparticle-modified epoxy is greater than that of the neat epoxy. The fatigue life enhancement of about three to four times in the nanoparticle-modified epoxy is observed over the entire range of stress levels investigated in the present work. Other investigations have shown that nanoparticle-modified epoxies exhibit higher fatigue life over their respective neat polymers [11,13].

The experimental data of stress vs. number of cycles to failure (S-N curves) for the bulk epoxies shown in Fig. 4 was fitted to Basquin's law [24]:

$$\sigma_{max} = \sigma_f' (N_f)^b \qquad (1)$$

where σ_f' is the fatigue strength coefficient (FSC), and b is the fatigue strength exponent (FSE). The values of the FSC and the FSE determined for the neat and the nanoparticle-modified epoxies are shown in Table 2. The addition of silica nanoparticles increases the FSC by about 34% and

decreases the FSE by about 16%. Zhou et al. [11] have observed a similar trend in the variation of fatigue properties in a carbon nanofibre-modified epoxy.

The fatigue fracture surfaces of the epoxies were sputter-coated with a thin layer of gold and observed using a scanning electron microscope (SEM). The SEM images of both the neat and the nanoparticle-modified epoxies are shown in Fig. 5. The neat epoxy shows a relatively smooth fracture surface, see Fig. 5(a), and is devoid of any indications of large-scale plastic deformation. However, the nanoparticle-modified epoxy exhibits a relatively rough fracture surface with presence of voids due to debonding of the silica nanoparticles, see Fig. 5(b). The measured void size was slightly greater than the diameter of the silica nanoparticles, indicating that plastic void growth had occurred during fatigue crack propagation and after the nanoparticles had debonded.

It has been observed that the fatigue crack growth rate of a silica nanoparticle-modified epoxy is over an order of magnitude lower than that of neat epoxy [14,25]. Previous work has shown that the fracture energy and fracture toughness are also increased by the addition of silica nanoparticles e.g. [4]. Several authors have considered the mechanisms by which the fracture toughness is increased. Rosso et al. [26] observed that the nanoparticles caused a high deflection of the crack growth, while Zhang et al. [27] observed that the nanoparticle induced dimples are likely to cause energy dissipation. However, Johnsen et al. [4] discounted the effect of crack deflection because the crack opening displacement in these materials is larger than the particle diameter. This does not satisfy the theory, which requires that the crack opening displacement is smaller than the particles. Ma et al. [5] proposed the initiation and development of a thin dilatation zone and nano-voids as the dominant toughening mechanisms. However, this mechanism seems unlikely due to the thickness of the samples and the constraint at the crack tip. Johnsen et al. [4] observed that nanoparticle debonding and the subsequent plastic void growth appeared to be the major toughening mechanism. From the present results it is clear that the fatigue life of epoxy was increased by the addition of 10 wt. % silica nanoparticles due to the particle debonding and plastic void growth mechanism.

3.2 Fatigue behaviour of GFRP composite

The stress-controlled, constant-amplitude, tension-tension fatigue test results for the GFRP composites with neat and 10 wt.% silica nanoparticle-modified epoxy matrices are shown in Fig. 6. It may be seen that the addition of silica nanoparticles enhances the fatigue life of the composite by about three to four times over the entire range of stress levels investigated. The fatigue properties (FSC and FSE) determined for the composites by fitting the S-N curve data (Fig. 6) to eqn. (1) are shown in Table 2. Once again, as observed in bulk epoxy but to a lesser extent, the FSC of GFRP composite increased, by about 13%, due to nanoparticle-modified epoxy matrix. However, unlike for the bulk epoxy, the FSE of the GFRP with the nanoparticle-modified epoxy matrix remained almost equal to that with the neat epoxy matrix.

The normalised stiffness variation with the number of cycles, evaluated for fatigue tests at σ_{max} = 150 MPa for the GFRP composites with the neat and nanoparticle-modified epoxy matrices is shown in Fig. 7. In general, both materials exhibit the typical stiffness reduction observed in FRP composites [22,28-32]. The three regions of the stiffness curve are clearly identifiable. It may be noted that the stiffness reduction in region I and region II is quite steep and significant for the neat GFRP composite when compared to that with the nanoparticle-modified matrix.

The typical transmitted light photographs showing the ±45° cracks in both composites, obtained after the application of 10000 fatigue cycles, are shown in Fig. 8. The ±45° crack density (CD) is shown in Fig. 9 as a function of the number of cycles. For both composites, the CD increased with the number of cycles and appears to saturate [33]. The saturation level of the CD was higher for the neat matrix, at about 4.5 mm^{-1}, than for the nanoparticle-modified matrix GFRP where it was about 2.8 mm^{-1}. This saturation level of the progressive formation of matrix cracks, which is also termed the characteristic damage state (CDS) [28,30,33], is reached more quickly for the neat matrix GFRP, in about 6000 cycles. The CDS appears to be delayed for the nanoparticle-modified matrix GFRP, and occurs at about 15000 cycles. It is clear from Fig. 9 that, for any given fatigue cycle, the GFRP with the neat matrix contains considerably more cracks than the GFRP with the nanoparticle-modified matrix, over the entire fatigue life of the composite.

The initiation and growth of interlaminar delaminations, particularly from the free edges of the test specimens was observed with continued fatigue cycling, see Fig. 10. Such free-edge delaminations have been previously observed in composite fatigue [34]. The visible delamination initiation was observed at about 6000 and 15000 cycles for the neat and nanoparticle-modified composites respectively. It may be noted that the CDS was reached after almost the same number of cycles for both composites. The further growth of such delaminations under fatigue leads to the final failure of the specimen.

Based on the results obtained, the sequence of fatigue damage development leading to final failure, and hence defining the fatigue life in a QI lay-up GFRP composite with and without a nanoparticle-modified matrix can be briefly described as follows [28,30,35,36]. Initially, in both GFRP composites, matrix cracks develop in the off-axis plies due to cyclic-fatigue loads, see Fig. 8. The density of these matrix cracks increases, see Fig.9, and the cracks propagate with further cyclic loading, resulting in a continuous decrease in the global stiffness of the composite (region I of Fig. 7). However, for the silica nanoparticle-modified matrix, the matrix cracking is suppressed and the crack density is lower, see Fig. 9. Also, from the bulk epoxy fatigue studies, it is clear that the fatigue life is enhanced due to the reduced crack growth rates in the nanoparticle-modified epoxy, see Figs. 4 and 5. It has been shown [14,25] that the fatigue crack growth rate for silica nanoparticle-modified epoxy is over an order of magnitude lower than that for neat epoxy. Thus reduced cracking results in reduced stiffness degradation of the GFRP with the nanoparticle-modified matrix compared to that with the neat matrix, see Fig. 7.

The matrix cracking process continues until the CDS is reached. From here the formation of secondary cracks in the epoxy matrix, perpendicular to the primary cracks, leads to initiation of delaminations, see Figs. 7 and 10. Growth of these delaminations leads to the continued stiffness loss in region II of Fig. 7. Once again the stiffness reduction is much slower in the nanoparticle-modified GFRP due to the reduced delamination/crack growth rates [14,25]. It has been shown that dispersive and matrix crack-coupled [30] fibre breakage is an additional fatigue damage mechanism which occurs during the entire fatigue life. We believe that such fibre breaks are delayed in the nanoparticle-modified GFRP due to the reduced crack growth rates. The

accumulation and growth of all these types of damage leads to final fatigue failure of the composite but the nanoparticle-modified matrix GFRP shows an improved fatigue life over that of the neat matrix.

4. Conclusions

The following conclusions may be drawn based on the results obtained in this investigation.

1. The fatigue life of 10 wt.% silica nanoparticle-modified bulk epoxy is about three to four times higher than that of neat epoxy. Silica nanoparticle debonding and subsequent plastic void growth absorb energy and contribute towards the enhanced fatigue life for the nanoparticle-modified epoxy.

2. The fatigue life of the GFRP composite with 10 wt.% silica nanoparticle-modified epoxy matrix is about three to four times higher than that of the GFRP with the neat epoxy matrix. The suppressed matrix cracking and reduced crack growth rate due to the particle debonding and plastic void growth mechanisms appears to contribute for the observed enhancement of the fatigue life in the GFRP with the nanoparticle-modified matrix.

Acknowledgements

Dr. CM Manjunatha wishes to thank and acknowledge the United Kingdom-India Education and Research Initiative (UKIERI) for the award of a Research Fellowship. He also wishes to thank Dr. AR Upadhya, Director, and Mr. DV Venkatasubramanyam, Head, STTD, National Aerospace Laboratories, Bangalore, India for permitting him to accept the Fellowship. The technical support staff and research students of the Department of Mechanical Engineering and the Composites Centre of the Aeronautics Department, Imperial College London are thanked for their assistance in the experimental work.

References

[1] Thostenson ET, Li C, Chou TW. Nanocomposites in context. Comp Sci Tech 2005; 65:491-516.

[2] Hussain F, Hojjati M, Okamoto M, Gorga RE. Polymer-matrix nanocomposites, processing, manufacturing, and application: an overview. J Comp Mater 2006; 40(17):1511-1575.

[3] Kinloch AJ, Mohammed RD, Taylor AC, Eger C, Sprenger S, Egan D. The effect of silica nanoparticles and rubber particles on the toughness of multiphase thermosetting epoxy polymers. J Mater Sci, 2005; 40(18):5083-5086.

[4] Johnsen BB, Kinloch AJ, Mohammed RD, Taylor AC, Sprenger S. Toughening mechanisms of nanoparticle-modified epoxy polymers. Polymer 2007; 48(2): 530-541.

[5] Ma J, Mo MS, Du XS, Rosso P, Friedrich K, Kuan HC. Effect of inorganic nanoparticles on mechanical property, fracture toughness and toughening mechanism of two epoxy systems. Polymer 2008; 49:3510-3523.

[6] Kinloch AJ, Mohammed RD, Taylor AC, Sprenger S, Egan DJ. The interlaminar toughness of carbon-fibre reinforced plastic composites using 'hybrid-toughened' matrices. J Mater Sci 2006; 41(15):5043-5046.

[7] Chisholm N, Mahfuz H, Rangari VK, Ashfaq A, Jeelani S. Fabrication and mechanical characterization of carbon/SiC-epoxy nanocomposites. Comp Struct 2005; 67(1):115-124.

[8] Kinloch AJ, Masania K, Taylor AC, Sprenger S, Egan D. The fracture of glass-fibre-reinforced epoxy composites using nanoparticle-modified matrices. J Mater Sci 2008; 43(3):1151-1154.

[9] Zheng Y, Zheng Y, Ning R. Effects of nanoparticles SiO_2 on the performance of nanocomposites. Mater Lett 2003; 57(19):2940-2944.

[10] Gojny FH, Wichmann, MHG, Fiedler B, Bauhofer W, Schulte K. Influence of nano-modification on the mechanical and electrical properties of conventional fibre-reinforced composites. Composites A 2005; 36(11):1525-1535.

[11] Zhou Y, Pervin F, Jeelani S. Mallick PK. Improvement in mechanical properties of carbon fabric-epoxy composite using carbon nanofibers. J Mater Proc Tech 2008; 198:445-453.

[12] Haque A, Shamsuzzoha M, Hussain F, Dean D. S2-glass/epoxy polymer nanocomposites: manufacturing, structures, thermal and mechanical properties. J Comp Mater 2003; 37(20):1821-1837.

[13] Zhou Y, Rangari V, Mahfuz H, Jeelani S, Mallik PK. Experimental study on thermal and mechanical behaviour of polypropylene, talc/polypropylene and polypropylene/clay nanocomposites. Mater Sci Eng A 2005; 402: 109-117.

[14] Blackman BRK, Kinloch AJ, Sohn Lee J, Taylor AC, Agarwal R, Schueneman G, Sprenger S. The fatigue and fracture behaviour of nano-modified epoxy polymers. J Mater Sci 2007; 42:7049-7051.

[15] Summerscales J, Searle TJ. Low-pressure (vacuum infusion) techniques for moulding large composite structures. Proc IMechE, J Mater Des Appl 2005; 219:45-58.

[16] Standard test method for tensile properties of plastics, ASTM D638-01, Annual book of ASTM Standards, American Society for Testing and Materials, PA, Vol. 8.02, 2003.

[17] Standard test method for tensile properties of polymer matrix composite materials, ASTM D3039, Annual book of ASTM Standards, American Society for Testing and Materials, PA, Vol. 15.03, 2003.

[18] Standard Test Method for Tension-Tension Fatigue of Polymer Matrix Composite Materials, ASTM D3479M-96, Annual book of ASTM Standards, American Society for Testing and Materials, PA, Vol. 8.02, 2003.

[19] Mandell JF, Meier U. Effect of stress ratio, frequency and loading time on the tensile fatigue of glass-reinforced epoxy, In: O'Brien TK, Ed., Long-Term Behaviour of Composites, ASTM STP 813, ASTM International, West Conshohocken, PA, 1983, pp. 55-77.

[20] Staff CR. Effect of load frequency and lay-up on fatigue life of composites. In: O'Brien TK, Ed., Long-Term Behaviour of Composites, ASTM STP 813, ASTM International, West Conshohocken, PA, 1983, pp. 78-91.

[21] Sun CT, Chan WS. Frequency effect on the fatigue life of a laminated composite, In.: Composite Materials: Testing and Design (Fifth Conference), ASTM STP 674, Tsai SW, Ed., ASTM International, West Conshohocken, PA, 1979, pp. 418-430.

[22] Lee J, Fu KE, Yang JN. Prediction of fatigue damage and life for composite laminates under service loading spectra. Comp Sci Tech 1996; 56:635-648.

[23] Gagel A, Lange D, Schulte K. On the relation between crack densities, stiffness degradation, and surface temperature distribution of tensile fatigue loaded glass-fiber non-crimp-fabric reinforced epoxy. Comp Part A 2006; 37:222-228.

[24] Buch, A. Fatigue Strength Calculation, Transtech Publications, Switzerland, 1988.

[25] Caccavale V, Wichmann M H.G., Quaresimin, M. Schulte K. (2007). Nanoparticle/Rubber Modified Epoxy Matrix Systems: Mechanical Performance in CFRPs. in: AIAS XXXVI Convegno Nazionale, Ischia, Napoli, 4-8 Sept 2007.

[26] Rosso P, Ye L, Friedrich K, Sprenger S. A toughened epoxy resin by silica nanoparticle reinforcement. J Appl Polym Sci 2006; 100(3):1849-1853.

[27] Zhang H, Zhang Z, Friedrich K, Eger C. Property improvements of in situ epoxy nanocomposites with reduced interparticle distance at high nanosilica content. Acta Mater 2006; 54(7):1833-1842.

[28] Talreja R. Fatigue of composite materials: damage mechanisms and fatigue life diagrams, Proc Roy Soc Lond A, 1989; 378:559-567.

[29] Hahn, HT, Kim RY. Fatigue behaviour of composite laminates. J Comp Mater 1976; 10:156-180.

[30] Case SW, Reifsnider KL. Fatigue of Composite Materials. In: Milne I, Ritchie RO, Karihaloo B. Eds., Comprehensive structural integrity. Vol. 4: Cyclic loading and fatigue, 1st edn. Elsevier Science, Amsterdam, 2003.

[31] Tate JS, Kelkar, AD. Stiffness degradation model for biaxial braided composites under fatigue loading. Composites B 2008; 39(3):548-555.

[32] Reifsnider KL, Jamison R. Fracture of fatigue-loaded composite laminate. Inter J Fat 1982; 4(4):187-197.

[33] Li C, Ellyin F, Wharmby A, On matrix crack saturation in composite laminates. Composites B 2003; 34:473-480.

[34] Case S W, Caliskan A, Iyengar N, Reifsnider KL. Performance simulation of high-temperature polymeric composite materials using MR Life. In: Proc ASME Aerosp Div-1996 ASME Int Mech Eng Cong Exp, pp. 375-380.

[35] Reifsnider K. Fatigue behaviour of composite materials, Int J Frac 1980; 16(6):563-583.

[36] Wharmby AW, Ellyin F, Wolodko JD. Observation on damage development in fiber reinforced polymer laminates under cyclic loading. Int J Fat 2003; 25:437-446.

Figure Captions

Fig. 1. Tapping-mode atomic force micrograph of 10 wt.% silica nanoparticle-modified bulk epoxy polymer.

Fig. 2. Schematic diagram showing the dimensions of the tensile and fatigue test specimens.

Fig. 3. Transmitted light photographs of GFRP composite with neat matrix showing the sequence of matrix crack development during fatigue loading.

Fig. 4. Stress vs. lifetime (S-N curves) for neat and 10 wt.% silica nanoparticle-modified bulk epoxy polymers.

Fig. 5. Scanning electron micrographs of the fatigue fracture surfaces of neat and 10 wt.% silica nanoparticle-modified bulk epoxy polymers. (Crack growth direction is from left to right; voids are circled).

Fig. 6. Stress vs. lifetime (S-N curves) for GFRP composite with neat and 10 wt.% silica nanoparticle-modified epoxy matrix.

Fig. 7. Normalised stiffness vs. number of cycles for GFRP composite with neat and 10 wt.% silica nanoparticle-modified epoxy matrix. (σ_{max} = 150 MPa).

Fig. 8. Transmitted light photographs showing matrix cracking for GFRP composites during fatigue loading. (σ_{max} = 150 MPa, N = 10000 cycles).

Fig. 9. Crack density of $\pm$45° cracks vs. number of fatigue cycles for GFRP composite with neat and 10 wt.% silica nanoparticle-modified matrix.

Fig. 10. Transmitted light photograph showing delaminations observed at the free edges of the specimen during fatigue testing of GFRP composite with neat matrix. (σ_{max} = 150 MPa).

Figures

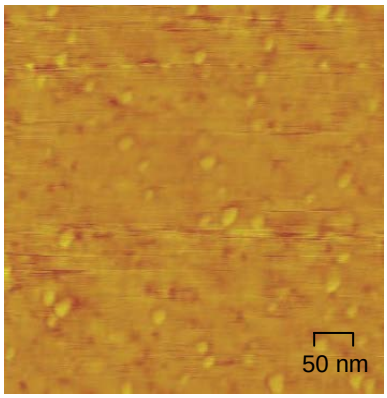

Fig. 1

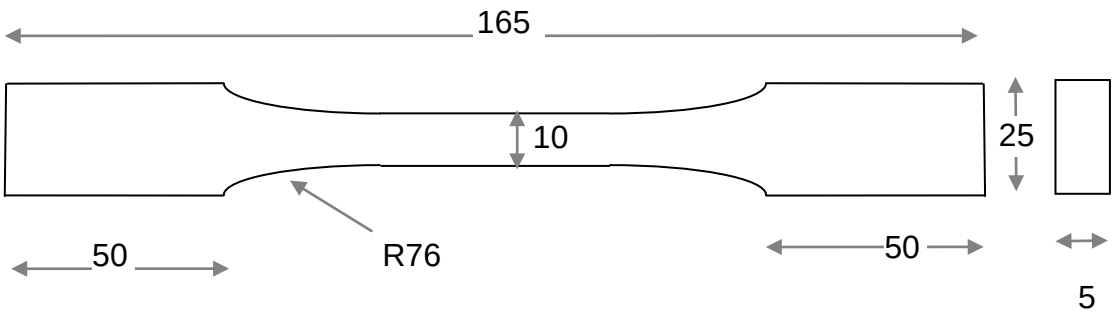

(a) Bulk epoxy polymer

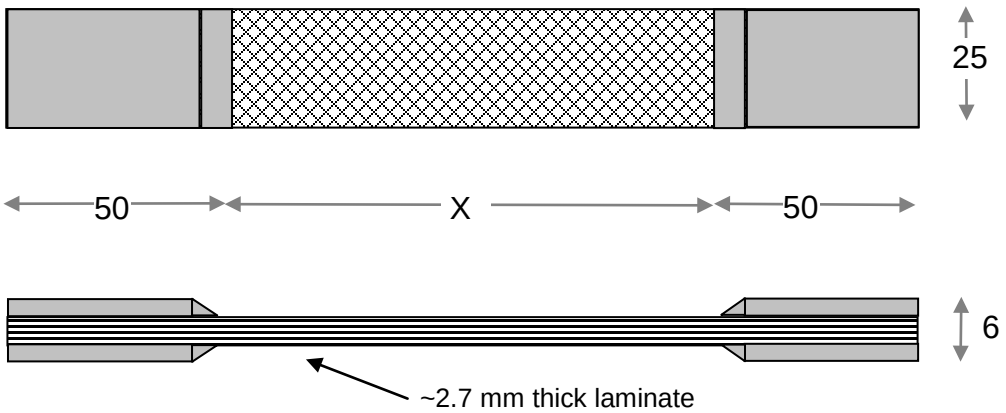

Note: All dimensions are in mm
X = 150mm for tensile tests
X = 50 mm for fatigue tests

(b) GFRP composite

Fig. 2.

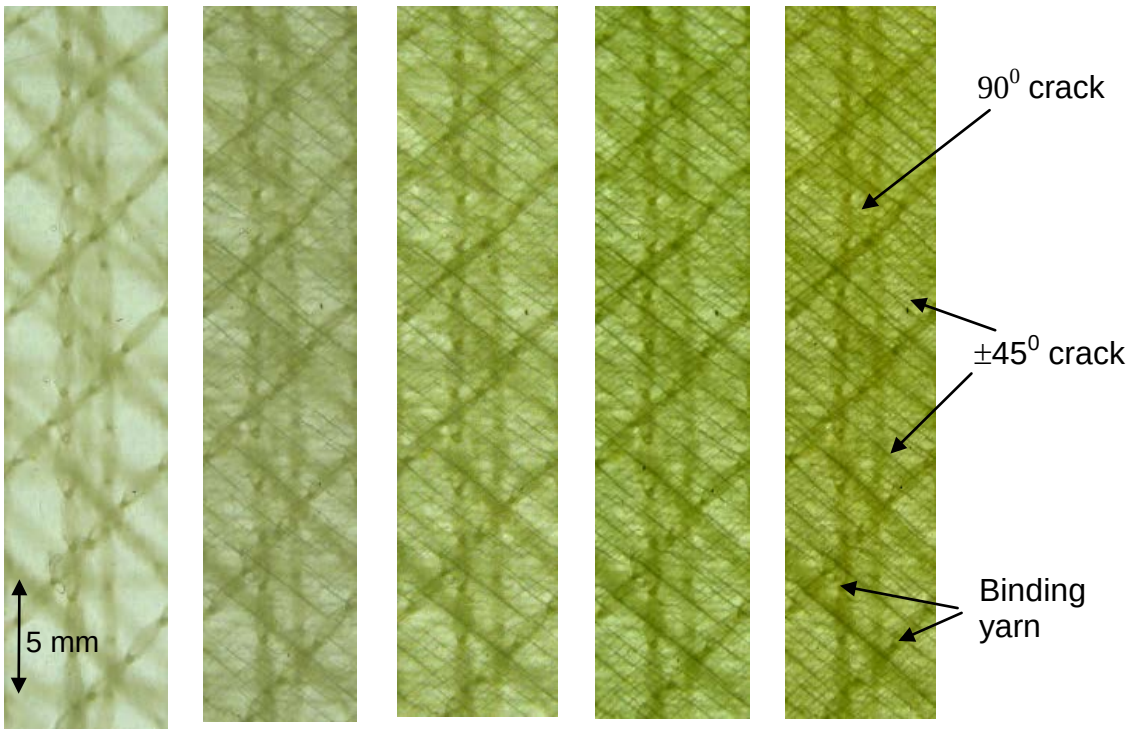
90⁰ crack
±45⁰ crack
Binding yarn
5 mm
N=0
N=1000
N=2000
N=4000
N=10000

Fig. 3.

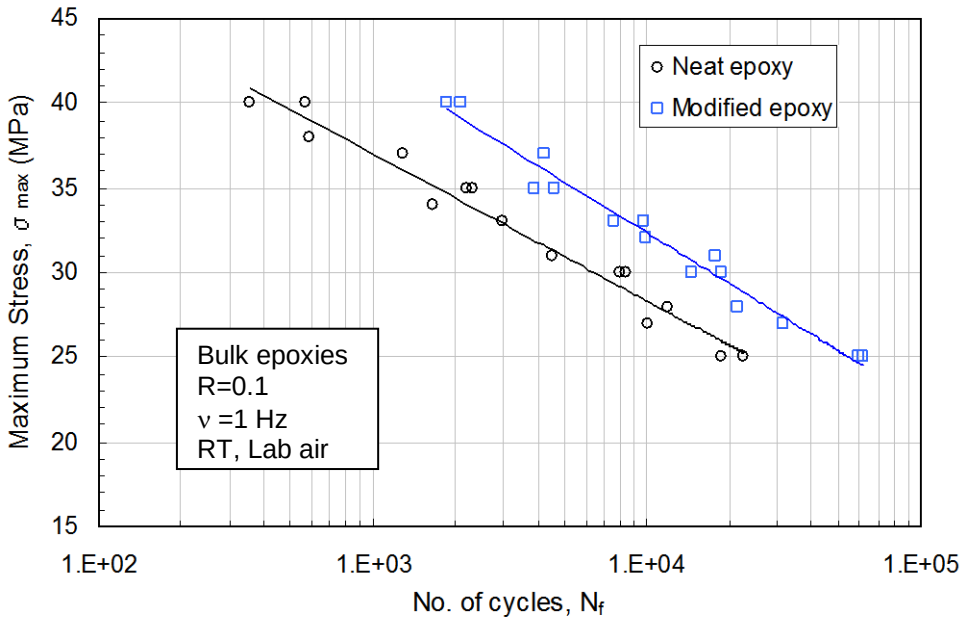
Neat epoxy
Modified epoxy
Bulk epoxies
R=0.1
ν =1 Hz
RT, Lab air
Maximum Stress, σ max (MPa)
No. of cycles, Nf
45
40
35
30
25
20
15
1.E+02
1.E+03
1.E+04
1.E+05

Fig. 4.

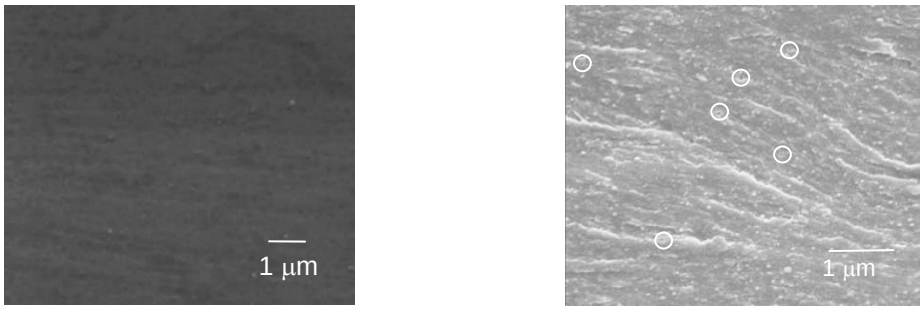

(a) Neat epoxy, σ_{max} = 37 MPa, (b) Modified epoxy, σ_{max} = 37 MPa,

Fig. 5.

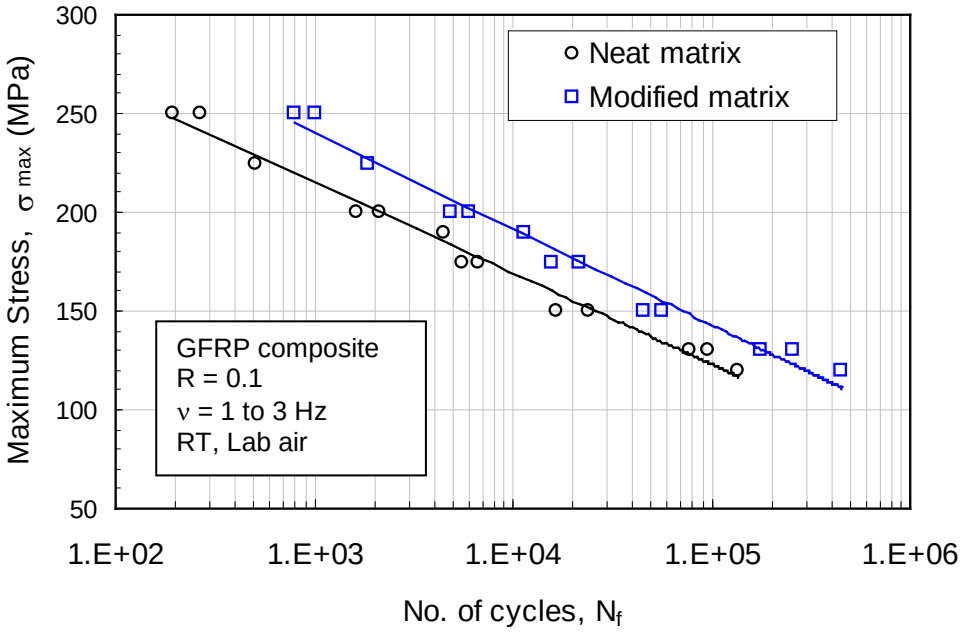

Fig. 6.

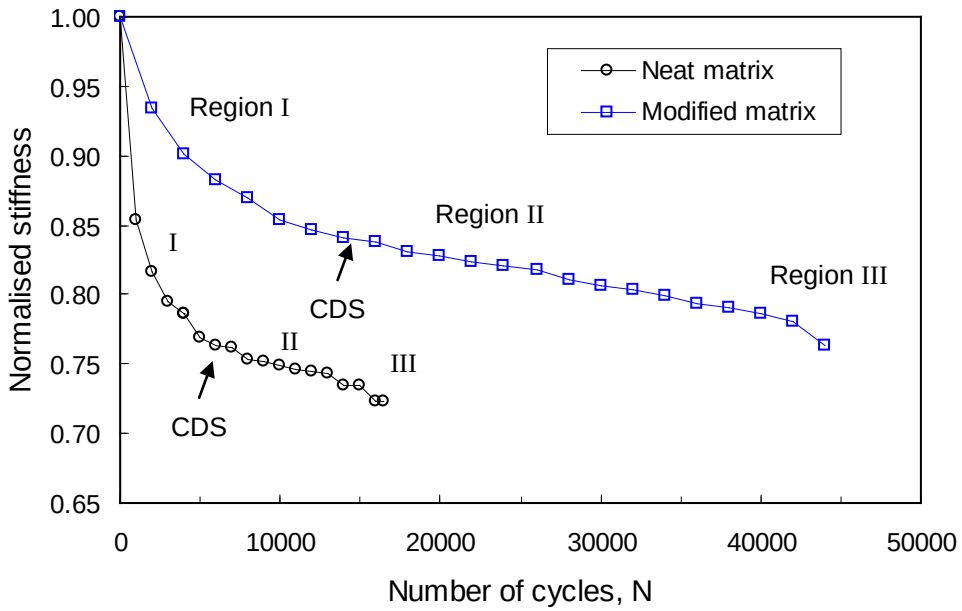

Fig. 7.

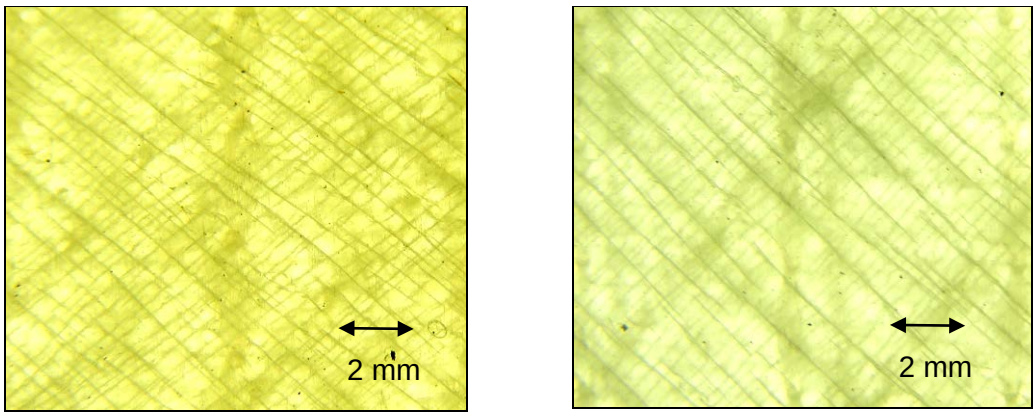

(a) GFRP-Neat matrix (b) GFRP-Modified matrix

Fig. 8.

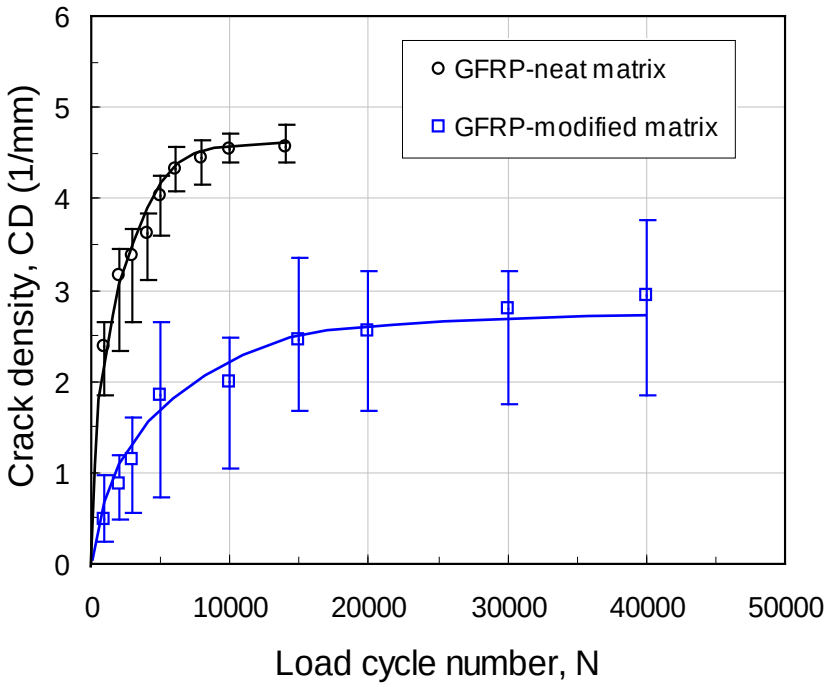
GFRP-neat matrix
GFRP-modified matrix
Crack density, CD (1/mm)
Load cycle number, N
0
1
2
3
4
5
6
0
10000
20000
30000
40000
50000

Fig. 9

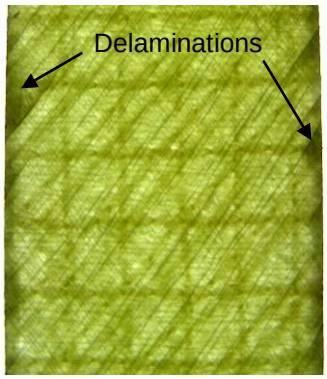
Delaminations

Fig. 10.

Tables

Table 1. Tensile properties of the bulk epoxies and the GFRP composites. Mean and standard deviation are quoted.

Material	Condition	Tensile Properties	
		UTS (MPa)	Modulus, E (GPa)
Bulk epoxy	Neat epoxy	73.3 ± 1.4	2.62 ± 0.05
	10 wt.% nanoparticle-modified epoxy	86.9 ± 1.3	3.07 ± 0.03
GFRP	Neat matrix	365 ± 13	17.5 ± 0.6
	10 wt.% nanoparticle-modified matrix	382 ± 12	18.8 ± 0.7

Table 2. Fatigue properties of the bulk epoxies and the GFRP composites.

Material	Condition	Fatigue properties	
		FSC (MPa)	FSE
Bulk epoxy	Neat epoxy	83.3	-0.117
	10 wt.% nanoparticle-modified epoxy	112	-0.136
GFRP	Neat matrix	462	-0.112
	10 wt.% nanoparticle-modified matrix	557	-0.119